IEEE Photonics Journal
An IEEE Photonics Society Publication

Open Access

CDMA RoFSO Links With Nonzero Boresight Pointing Errors Over *M* Turbulence Channels

Volume 10, Number 5, October 2018

Michalis P. Ninos
Hector E. Nistazakis
Harilaos G. Sandalidis
George S. Tombras, *Senior Member, IEEE*

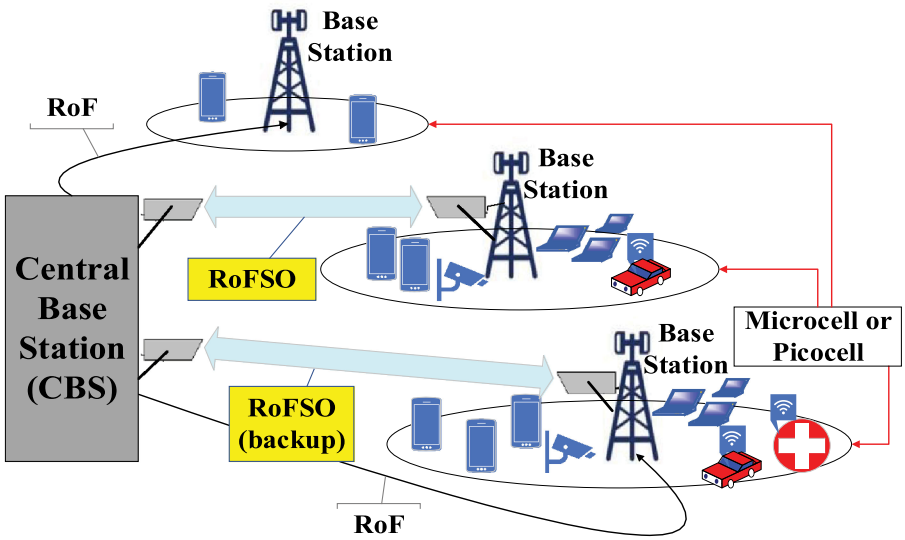

DOI: 10.1109/JPHOT.2018.2856369
1943-0655 © 2018 IEEE

CDMA RoFSO Links With Nonzero Boresight Pointing Errors Over *M* Turbulence Channels

Michalis P. Ninos,[1] **Hector E. Nistazakis**,[1]
Harilaos G. Sandalidis,[2]
and George S. Tombras,[1] ***Senior Member, IEEE***

[1]Department of Electronics, Computers, Telecommunications and Control, Faculty of Physics, National and Kapodistrian University of Athens, Athens 15784, Greece
[2]Department of Computer Science and Biomedical Informatics, University of Thessaly, Volos 38221, Greece

DOI:10.1109/JPHOT.2018.2856369

Manuscript received May 10, 2018; revised July 4, 2018; accepted July 11, 2018. Date of publication July 19, 2018; date of current version August 1, 2018. This work was supported by the European Union's Horizon 2020 research and innovation program under Grant 777596. Corresponding author: Hector E. Nistazakis (e-mail: enistaz@phys.uoa.gr).

Abstract: Radio-on-Free-Space Optical systems constitute a very attractive option for interconnecting central base stations with remote antenna units. Nonetheless, the optical signal propagation through the atmosphere is tremendously affected by turbulence- and misalignment-induced fading. In the present study, we investigate the transmission of code division multiple access signals over a free-space optical (FSO) link. The atmospheric turbulence is modeled by the *M* (Malaga) distribution, which acts as a unifying statistical model encompassing all the well-known distributions that have been proposed in the FSO area. In addition, nonzero boresight pointing errors (PEs) are employed, which are described by an accurate approximation of the Beckmann distribution. Novel mathematical expressions are extracted regarding the average bit error rate and the outage probability of the forward and the reverse link. Moreover, appropriate numerical results are depicted for various turbulence and PE scenarios, along with their associated corroborative outcomes.

Index Terms: Radio on FSO (RoFSO), code division multiple access (CDMA), atmospheric turbulence, nonzero boresight pointing errors (PEs).

1. Introduction

Radio over fiber (RoF) systems have been considered as the prominent solution for transferring radio frequency (RF) signals from central base stations (CBS) to remote antenna units (RAUs) or simply base stations (BS) in micro/picocellular radio architectures. However, in case the expenditure on installing fiber cables is high, radio-on-free-space optical (RoFSO) technology can be utilized as a viable and alternative choice [1]. A potential RoFSO deployment in the 5G cellular architecture is visualized in Fig. 1. A popular and well employed wireless standard is the code division multiple access (CDMA) scheme based on the spread-spectrum technique, where multiple users can communicate simultaneously using the same bandwidth. The cellular mobile communications standards of IS-95, IS-2000, and UMTS are based on the CDMA technology. Also, WLAN services such as IEEE 802.11b use the CDMA technique [2]. Another point in favor of CDMA signals

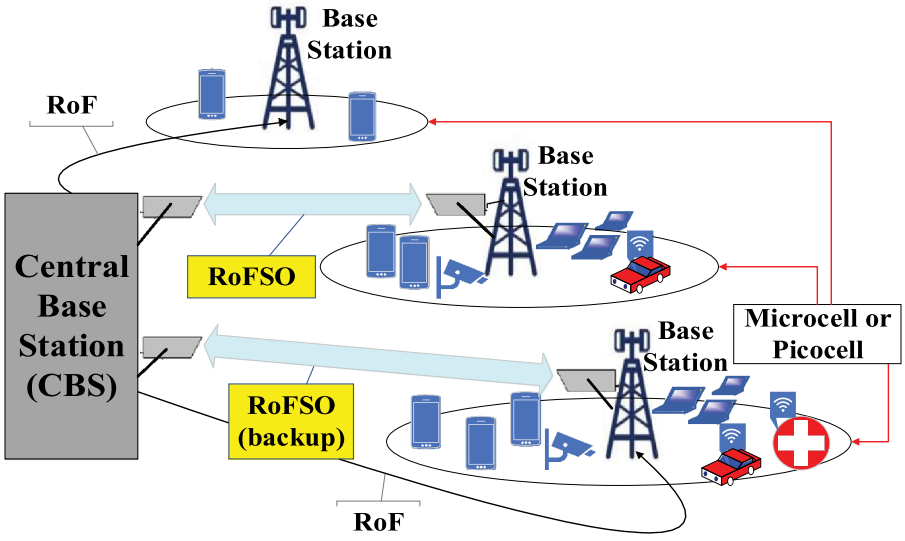

Fig. 1. A potential scenario for RoFSO deployment in the 5G cellular architecture.

is that they require less dynamic range in contrast to OFDM signals, rendering them suitable for RoF and RoFSO links [3]. However, the multiple access interference (MAI) limits the performance of CDMA systems [2]. Moreover, the propagation of the optical signals through the free-space suffers from severe atmospheric-related issues including turbulence and pointing error (PE) effects [4], [5].

Several efforts have been carried out on the application of RoFSO systems for RF signal transmission and especially for CDMA signals. In [6], Bekkali *et al.* assumed a subcarrier multiplexed (SCM) RoFSO link based on CDMA where the average bit error rate (ABER) metric is evaluated over gamma-gamma fading channels. In [7], Naila *et al.* estimated the outage probability (OP) of CDMA signal transmission over FSO links using an aperture averaging technique over log-normal fading. In [8], a CDMA-based RoFSO link was theoretically and experimentally evaluated indicating acceptable performance under various turbulence conditions. However, the above works confined their study on the reverse (uplink) direction. The forward direction of a CDMA RoFSO link was investigated in [9] with the ABER evaluation for each user, restricted though to weak and moderate turbulence regime modelled by the Gamma distribution along with nonzero boresight PE. Lastly, an OFDM RoFSO link with QAM or PSK modulation was thoroughly analyzed in [10], where Nistazakis *et al.* examined the ABER and OP performance over the *M*-turbulence, taking account of nonlinearities related to multiple closely-spaced orthogonal subcarriers without PE influence.

In the current paper, we investigate a CDMA RoFSO point-to-point link (P2P) in both directions of the forward (downlink) link and the reverse link. It is vital, also, to evaluate the performance on the forward link, since the atmospheric medium poses significant limitations on optical wireless signal transmission. The P2P link is impaired by turbulence in conjunction with nonzero boresight (NB) PEs. A statistical turbulence model called *M* (Malaga) is assumed having the additional feature of unifying all the previous and well-studied distributions in the FSO context such as the log normal, the gamma gamma, the *K*, the negative exponential, etc. [4]. Moreover, a generalized PE model is employed, which takes account of the NB displacement of the optical beam center from the receiver center. Along with the boresight displacement, different spatial jitters are considered for the elevation and the horizontal axis. This mathematical tractable model is an approximation of the Beckmann PDF and is described by a modified Rayleigh distribution [5]. Novel mathematical expressions are obtained for the estimation of the ABER and the OP of the link.

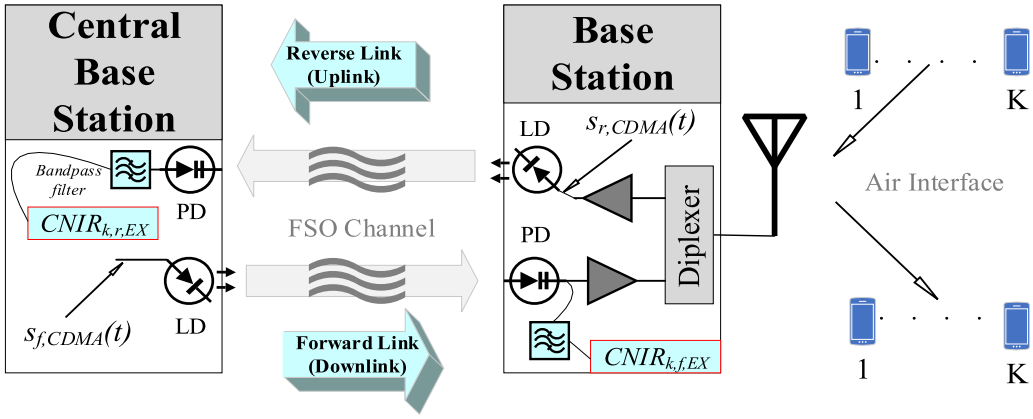

Fig. 2. The block diagram of the CDMA RoFSO system for both directions of the forward and the reverse link.

2. The CDMA RoFSO Link

2.1 Forward Link

In this section, we consider the forward (downlink) CDMA RoFSO link for the distribution of K mobile users' signals with destination from the CBS to the RAU. At the CBS we assume a synchronous transmission for the K active users (Fig. 2). In this vein, the $s_{f,CDMA}(t)$, which is used to directly modulate the optical intensity of the transmitter laser diode (LD), can be expressed as [2, Eq. (6.32)]

$$s_{f,CDMA}(t) = \sum_{k=1}^{K} s_k(t) = \sum_{k=1}^{K} C_k(t)\, d_k(t) \cos(\omega_c t + \phi_0), \tag{1}$$

where $\omega_c = 2\pi f_c$ is the RF carrier angular frequency, φ_0 is the initial phase, $d_k(t) = \sum_{m=-\infty}^{+\infty} d_m^{(k)} P_{T_b}(t - mT_b)$ is the user's data stream with $d_m^{(k)}$ taking the binary values ± 1 with equal probability in the interval $[mT_b, (m+1)T_b]$.The T_b is the user's data bit duration and P_{T_b} is a rectangular pulse which equals unity for $0 \le t \le T_b$ and zero otherwise. The parameter $C_k(t)$ is the code sequence equal to $C_k(t) = \sum_{n=-\infty}^{+\infty} c_n^{(k)} P_{T_c}(t - nT_c)$ with $c_n^{(k)}$ taking the values ± 1 with equal probability in the interval $[mT_c, (m+1)T_c]$ where P_{T_c} is again a rectangular pulse equal to unity in the interval $0 \le t \le T_c$ and zero otherwise. The spreading factor, i.e., processing gain is defined as $G_p = T_b/T_c$, which determines to a certain degree the upper limit of the total number of users that can support a given BS.

Due to the nonlinear response of the laser diode (LD), harmonics and inter-modulation (IMD) products are generated. Thus, the transmitted optical power from the CBS to the RAU is expressed through the nonlinear expression [3, Eq. (2.1)]

$$P_t(t) = P_0 \left[1 + \sum_{k=1}^{K} m_k s_k(t) + a_2 \left(\sum_{k=1}^{K} m_k s_k(t) \right)^2 + a_3 \left(\sum_{k=1}^{K} m_k s_k(t) \right)^3 \right], \tag{2}$$

where P_0 is the average transmitted optical power, m_k represents the optical modulation index (OMI) or optical modulation depth (OMD) for each user, and $\alpha_{2,}, \alpha_3$ are the second and third-order nonlinear coefficients. Intensity modulation with direct detection (IM/DD) is employed for the FSO link and the received optical power at the p-i-n photo-detector (PD) input is described as [6]

$$P_r(t) = P_t(t) L_{tot} I + n(t), \tag{3}$$

where L_{tot} encompasses the total losses of the optical signal due to path loss, geometrical loss etc., $n(t)$ stands for the additive white Gaussian noise (AWGN) from the air interface, while I is the total

normalized instantaneous irradiance on the receiver side. It is given as a product of two random variables I_t and I_p, i.e., $I = I_t I_p$ where I_t represents the normalized irradiance for the atmospheric turbulence while I_p corresponds to the PE effect.

In single-octave systems only 3rd order IMD (IMD3) products fall in the signal bandwidth. Thus, the photo-induced current at the PD output after the bandpass filter is given as [6]

$$i(t, I) \approx I_{ph}\left[1 + \sum_{k=1}^{K} m_k s_k(t) + a_3\left(\sum_{k=1}^{K} m_k s_k(t)\right)^3\right] + n_{opt}(t), \tag{4}$$

where $I_{ph} = \rho L_{tot} P_0 I$ stands for the dc value of the received photocurrent, ρ is the responsivity of the PD, and n_{opt} is the optical link noise with power spectral density (PSD) N_0. The PSD N_0 is a sum of three factors, two of them related to the photo-detection and are the thermal noise and the shot noise, and the last one related to the LD relative intensity noise (*RIN*) [3]. Thus, N_0 is given as

$$N_0 = N_{th} + N_{shot} + N_{RIN} = \frac{4K_B T}{R_L} + 2qI_{ph} + {I_{ph}}^2 (RIN)\left(1 + \sum_{k=1}^{K} m_k^2 \left\langle s_k^2(t)\right\rangle\right), \tag{5}$$

where K_B is the Boltzmann's constant, T is the absolute temperature, R_L is the receiver circuit load resistor, q is the electron charge, and *RIN* is the relative intensity noise process, which is proportional to the square of the optical power. It is worth mentioning that we employ a new expression for the *RIN*, which includes its dynamic behaviour, i.e., its dependency on the modulating signal strength *s(t)* and the number of subcarriers. The validity of this expression is presented in [3, Ch. 4].

On the forward link, due to the synchronous transmission of the K CDMA signals, the MAI is minimized. Thus, only IMD and clipping noise are significant noise sources except for the optical link noise [3]. In [11], an expression for the variance of the IMD3 was derived. However, in this expression MAI is taken into account due to the asynchronous transmission on the reverse link. Thus, in the [11, Eq. (12)] the terms $\tilde{I}_2 \rightarrow \tilde{I}_6$ consist of the quantities $r_{k,1}$, $r_{j,k}$, $r_{i,j,k}$, which correspond to cross-correlation products between the code sequences of different users [12]. Since the transmission is synchronous, orthogonality among the CDMA user's codes is maintained and thus the cross-correlation is zero [2]. Hence, these terms are dropped and the expression for the IMD3 in [11] reduces to

$$\sigma^2_{IMD,k} = \frac{9\alpha_3^2 m_k^6 (K - 1) I_{ph}^2}{128}. \tag{6}$$

Along with IMD3, the clipping noise power is given from the following expression [8]

$$\sigma^2_{cl,k} = \frac{I_{ph}^2 m_k^6 K^3}{27.2} \exp\left(-\frac{1}{2m_k^2 K}\right). \tag{7}$$

In this way, the total nonlinear distortion on the forward link $n_{NLD,f,k}$ is given as the sum of the above-mentioned noise factors i.e., $n_{NLD,f,k} = \sigma^2_{IMD,k} + \sigma^2_{cl,k}$. Hence, the carrier to noise plus interference ($CNIR_k$) power ratio for the k_{th} user's signal on the forward link is evaluated as [3], [6]

$$CNIR_{k,f}(I) = \frac{\left(m_k I_{ph}\right)^2}{2\left(N_0 B + n_{NLD,f,k}\right)}, \tag{8}$$

where B is the receiver's bandpass filter bandwidth centered at the RF carrier f_c. Following the same steps as presented in [6]–[8] and taking the average value of the total noise over the total instantaneous normalized irradiance I, we conclude to

$$CNIR_{k,f}(I) \approx \frac{\left(m_k \rho L_{tot} P_0 I\right)^2}{2\left(\langle N_0 B\rangle_{AV} + \left\langle n_{NLD,f,k}\right\rangle_{AV}\right)}, \tag{9}$$

with the corresponding expected value of $CNIR_k$ being equal to

$$CNIR_{k,f,EX} \approx \frac{(m_k \rho L_{tot} P_0 E[I])^2}{2\left(\langle N_0 B\rangle_{AV} + \langle n_{NLD,f,k}\rangle_{AV}\right)}, \tag{10}$$

where $E[.]$ denotes the average value of the total normalized irradiance, which is presented in Section 3.

2.2 Reverse Link

On the reverse (uplink) link, multiple CDMA signals from K mobile users arrive at a specific BS (Fig. 2), which are detected and added asynchronously. A power control mechanism is employed, so the transmitted power from each mobile user arrives at the BS with the same power. The total received signal $s_{r,CDMA}(t)$ at the BS from K users accessing the network is expressed as [2], [8]

$$s_{r,CDMA}(t) = \sum_{k=1}^{K} s_k(t-\tau_k) = \sum_{k=1}^{K} C_k(t-\tau_k)\, d_k(t-\tau_k)\cos(\omega_c t + \phi_k), \tag{11}$$

where τ_k is the access delay of the k_{th} user with $0 \le \tau_k \le T_b$, d_k is the data sequence, C_k the coded waveform, and φ_k represents the initial phase shift, which is used from the k_{th} user, plus shift due to the access delay. In the analysis and for simplicity reasons we assume negligible additive background noise and Rayleigh fading from the air interface. After the detection process at the BS the total signal is amplified to reach the appropriate current level and then is used to modulate the optical intensity of the LD.

The LD from the BS emits the optical signal that propagates through the atmospheric turbulent medium. At the CBS the detected $CNIR_k(I)$ is given as

$$CNIR_{k,r}(I) = \frac{(m_k I_{ph})^2}{2(N_0 B + n_{NLD,r,k})}, \tag{12}$$

where all the parameters m_k, I_{ph}, N_0, and B are the same as on the forward link. The nonlinear distortion on the reverse link $n_{NLD,r,k}$ is a sum of three factors which are the IMD3 noise, the clipping noise given from (7) and one additional term due to the generated MAI. The IMD3 for the case of the reverse link and the generated MAI from K-1 other active users are given through the following expressions [8], [11]

$$\sigma^2_{IMD,r,k} = \frac{(m_k I_{ph})^2}{2}\left[\frac{\alpha_3 m_k^2 (2K-1)(K-1)}{8G_p} + \frac{\alpha_3^2 m_k^4 (K-1)}{64}\left(9 + \frac{252K^2 + 300K - 648}{10G_p}\right)\right], \tag{13}$$

$$\sigma^2_{MAI,k} = (m_k I_{ph})^2 \frac{K-1}{12G_p}. \tag{14}$$

Thus, the total $n_{NLD,r,k}$ is given as $n_{NLD,r,k} = \sigma^2_{IMD,r,k} + \sigma^2_{cl,k} + \sigma^2_{MAI,k}$ and the $CNIR_k(I)$ on the reverse link, following the same methodology as presented in the previous section, is evaluated as

$$CNIR_{k,r}(I) \approx \frac{(m_k \rho L_{tot} P_0 I)^2}{2\left(\langle N_0 B\rangle_{AV} + \langle n_{NLD,r,k}\rangle_{AV}\right)}, \tag{15}$$

with the expected value of $CNIR_{k,r,EX}$ being equal to

$$CNIR_{k,r,EX} \approx \frac{(m_k \rho L_{tot} P_0 E[I])^2}{2\left(\langle N_0 B\rangle_{AV} + \langle n_{NLD,r,k}\rangle_{AV}\right)} \tag{16}$$

3. Channel Model

In the Kolmogorov theory of turbulence, the Rytov variance for plane wave propagation is given as $\sigma_R^2 = 1.23 C_n^2 k^{7/6} L_S^{11/6}$. This parameter quantifies the turbulence strength. The parameter C_n^2 is the refractive index structure parameter and its value ranges from 10^{-17} $m^{-2/3}$ up to 10^{-13} $m^{-2/3}$ for weak to strong turbulence conditions. The parameter $k = 2\pi/\lambda$ is the optical wavenumber with λ being the transmitted optical wavelength and L_S is the link distance. When $\sigma_R^2 < 1$ the irradiance fluctuations are categorized as weak, while for $\sigma_R^2 \sim 1$ the irradiance fluctuations are characterized as moderate. When $\sigma_R^2 > 1$ the optical signal experiences strong irradiance fluctuations and in the limiting case of $\sigma_R^2 \to \infty$ we have the saturation regime [13].

The closed-form expression for the combined PDF of the *M*-distributed turbulence with the Rayleigh distribution PE model is derived in [14]. The modified Rayleigh distribution has the same PDF with the only difference that the ξ and A_0 parameters are replaced by the ξ_{mod} and A_{mod} respectively. Thus, the combined statistical channel model for the *M*-turbulence with the modified Rayleigh distribution can be derived in a similar manner, and its PDF is

$$f_{comb,I}(I) = \frac{\xi^2_{\text{mod}}\, A^{(\aleph \text{ or } \Re)}}{2} I^{-1} \sum_{j=1}^{(\aleph \text{ or } \Re)} a_j^{(\aleph \text{ or } \Re)} \left(B^{(\aleph \text{ or } \Re)}\right)^{-\frac{\alpha+j}{2}} G_{1,3}^{3,0}\left(B^{(\aleph \text{ or } \Re)} \frac{I}{A_{\text{mod}}} \,\middle|\, \begin{matrix} \xi^2_{\text{mod}} + 1 \\ \xi^2_{\text{mod}},\ \alpha,\ \beta \end{matrix}\right), \quad (17)$$

where $G_{p,q}^{m,n}[\cdot]$ is the Meijer G-function [15, eq. (9.301)]. This mathematical form is divided in two cases which depend on the value of the β parameter. When the β parameter is a natural number, i.e., $\beta \in \aleph$, then the summation in (17) becomes $\sum_{(\aleph)}[.] = \sum_{j=1}^{\beta}[.]$ and the parameters $A^{(\aleph)}$, $a_j^{(\aleph)}$ and $B^{(\aleph)}$ are given through the expressions, $A^{(\aleph)} = \left(2\alpha^{\alpha/2}(\gamma\beta)^{\beta+\frac{\alpha}{2}}\right) / \left(\gamma^{(2+\alpha)/2}\Gamma(\alpha)(\gamma\beta+\Omega')^{\beta+\frac{\alpha}{2}}\right)$, $a_j^{(\aleph)} = \binom{\beta-1}{j-1} \frac{(\gamma\beta+\Omega')^{1-\frac{j}{2}}}{(j-1)!} \left(\frac{\Omega'}{\gamma}\right)^{j-1} (\frac{\alpha}{\beta})^{j/2}$, $B^{(\aleph)} = \frac{\alpha\beta}{\gamma\beta+\Omega'}$ where $\binom{\beta}{j}$ is the binomial coefficient and $\Gamma(.)$ is the gamma function.

In the case when β is a real number i.e., $\beta \in \Re$,the summation in (17) takes the form $\sum_{(\Re)}[.] = \sum_{j=1}^{\infty}[.]$ and the parameters $A^{(\Re)}$, $a_j^{(\Re)}$ and $B^{(\Re)}$ are given through the expressions, $A^{(\Re)} = (2\alpha^{\alpha/2}(\gamma\beta)^{\beta}) / (\gamma^{(2+\alpha)/2}\Gamma(\alpha)(\gamma\beta+\Omega')^{\beta})$, $a_j^{(\Re)} = \frac{(\beta)_{j-1}(\alpha\gamma)^{j/2}}{[(j-1)!]^2 \gamma^{j-1}(\gamma\beta+\Omega')^{j-1}}$, $B^{(\Re)} = \alpha/\gamma$ where $(\beta)_j$ represents the Pochhammer symbol.

The parameter α of the *M* distribution is a positive parameter and corresponds to the effective number of large-scale eddies of the scattering process, β is a parameter related to small-scale fluctuations, and the parameter γ is given as $\gamma = 2b_0(1-\rho)$. The quantity $2b_0$ is the average power of the total scatter components and ρ fulfils the inequality $0 \le \rho \le 1$ and quantifies the amount of scattering power coupled to the LOS component. Finally, Ω' corresponds to the average power from the coherent contributions and is calculated as $\Omega' = \Omega + \rho 2b_0 + 2\sqrt{2b_0\Omega\rho}\cos(\phi_A - \phi_B)$ with φ_A, φ_B being the deterministic phases of the LOS and the coupled to LOS components [4].

Moreover, the parameter ξ_{mod} is given as $\xi_{\text{mod}} = W_{z,eq}/2\sigma_{\text{mod}}$ with the parameter σ_{mod} being equal to [5]

$$\sigma_{\text{mod}} = \left(\frac{3\mu_x^2\sigma_x^4 + 3\mu_y^2\sigma_y^4 + \sigma_x^6 + \sigma_y^6}{2}\right)^{1/6}, \quad (18)$$

with σ_x, and σ_y being the standard deviations on the horizontal and the elevation axis and μ_x, μ_y being the fixed boresight errors of the optical beam center from the center of the receiver for the two vertical axes. Next, the parameter A_{mod}, is assessed as [5]

$$A_{\text{mod}} = A_0 \exp\left(\frac{1}{\xi^2_{\text{mod}}} - \frac{1}{2\xi_x^2} - \frac{1}{2\xi_y^2} - \frac{\mu_x^2}{2\sigma_x^2\xi_x^2} - \frac{\mu_y^2}{2\sigma_y^2\xi_y^2}\right), \quad (19)$$

where $\xi_x = W_{z,eq}/2\sigma_x$ and $\xi_y = W_{z,eq}/2\sigma_y$ with $W_{z,eq}$ being the equivalent beam radius at the receiver and is given through the expression $W_{z,eq}^2 = \sqrt{\pi} erf(\upsilon) W_z^2 / 2\upsilon \exp(-\upsilon^2)$, $A_0 = [erf(\upsilon)]^2$,

$\upsilon = \sqrt{\pi} D / 2\sqrt{2} W_z$ with D being the receiver aperture diameter, while W_z is the Gaussian beam waist on the receiver plane. The W_z is evaluated by the initial beam waist at the transmitter W_0, the C_n^2 parameter, and the link distance L_S [16].

Lastly, the expected value of the total instantaneous irradiance I i.e $E[I] = \int_0^\infty I \, f_{comb,I}(I) dI$ when β is a natural number is obtained as [17]

$$E[I]^{\aleph} = \frac{\xi_{\text{mod}}^2 \, A_{\text{mod}}}{\xi_{\text{mod}}^2 + 1} \left(\gamma + \Omega'\right), \tag{20}$$

while, when β is a real number is given as [14]

$$E[I]^{\Re} = \frac{\xi_{\text{mod}}^2 \, A_{\text{mod}}}{\xi_{\text{mod}}^2 + 1} \frac{\Gamma(\alpha+1)}{\Gamma(\alpha)\,\alpha} \left(\frac{\gamma\beta}{\gamma\beta + \Omega'}\right)^{\beta} \gamma \, \Gamma(2) \, {}_2F_1\left(2, \beta; 1; \frac{\Omega'}{\gamma\beta + \Omega'}\right), \tag{21}$$

where ${}_2F_1(a, b; c; x)$ is the Gaussian hypergeometric function [15, eq. (9.100)].

3. Performance Analysis

3.1 Average Bit Error Rate

Assuming that the RF signals, for each kth user, are modulated with an M-QAM modulation, the conditional bit error rate (BER) is given as [10]

$$P_{b,k} = \frac{\left(1-\sqrt{M^{-1}}\right)}{\log_2(M)} \left[2erfc\left(\sqrt{\frac{3CNIR_k(I)}{2(M-1)}}\right) - \left(1-\sqrt{M^{-1}}\right) erfc^2\left(\sqrt{\frac{3CNIR_k(I)}{2(M-1)}}\right)\right]. \tag{22}$$

Thus, taking account of the combined statistical channel model derived in the previous section, the ABER performance for the kth user's signal is estimated as [10]

$$P_{b,k,Av} = \frac{\left(1-\sqrt{M^{-1}}\right)}{\log_2(M)} \int_0^\infty \left[2erfc\left(\sqrt{\frac{3CNIR_k(I)}{2(M-1)}}\right) - \left(1-\sqrt{M^{-1}}\right) erfc^2\left(\sqrt{\frac{3CNIR_k(I)}{2(M-1)}}\right)\right] f_{comb,I}(I)\, dI, \tag{23}$$

where the $CNIR_k(I)$ is given either from (9) or (15) for the cases of the forward or the reverse link transmission, respectively. Using an approximation formula for the *erfc(.)* given in [18] as $erfc(x) \approx 1/6e^{-x^2} + 1/3e^{-4x^2} + 1/3e^{-4x^2/3}$, the integral in (23) becomes

$$\begin{aligned} P_{b,k,Av} = \frac{\left(1-\sqrt{M^{-1}}\right)}{\log_2(M)} \int_0^\infty \Bigg[& 2erfc\left(\sqrt{\frac{3CNIR_k(I)}{2(M-1)}}\right) - \frac{1}{9}\left(1-\sqrt{M^{-1}}\right)\left(\frac{1}{4}\, e^{-\frac{3CNIR_k(I)}{(M-1)}} + e^{-\frac{15CNIR_k(I)}{2(M-1)}} + \right. \\ & \left. + e^{-\frac{12CNIR_k(I)}{(M-1)}} + e^{-\frac{7CNIR_k(I)}{2(M-1)}} + 2e^{-\frac{8CNIR_k(I)}{(M-1)}} + e^{-\frac{4CNIR_k(I)}{(M-1)}}\right)\Bigg] f_{comb,I}(I)\, dI \end{aligned} \tag{24}$$

Hence, by replacing the combined PDF of the M-turbulence with NB PEs given in (17), substituting for the exponential terms with the equality $\exp(z) = G_{0,1}^{1,0}(-z|0)$ and using the formula from [19, eq. (21)], the following closed-form mathematical expression is obtained

$$\begin{aligned} P_{b,k,Av} = \frac{\left(1-\sqrt{M^{-1}}\right)\xi_{\text{mod}}^2 \, A^{(\aleph \text{ or } \Re)}}{\log_2(M)} \sum_{j=1}^{(\aleph \text{ or } \Re)} \Bigg\{ & a_j^{(\aleph \text{ or } \Re)} \left(B^{(\aleph \text{ or } \Re)}\right)^{-\frac{\alpha+j}{2}} \frac{2^{\alpha+j-3}}{\pi} \left[\frac{1}{\sqrt{\pi}} \Phi_{j,k} - \right. \\ & \left. - \frac{1}{18}\left(1-\sqrt{M^{-1}}\right)\left(\frac{1}{4}\Psi_{j,k}(2) + \Psi_{j,k}(5) + \Psi_{j,k}(8) + \Psi_{j,k}\left(\frac{7}{3}\right) + 2\Psi_{j,k}\left(\frac{16}{3}\right) + \Psi_{j,k}\left(\frac{8}{3}\right)\right)\right]\Bigg\}, \end{aligned} \tag{25}$$

where

$$\Omega_k = \frac{24CNIR_{k,EX}}{(M-1)} \left(\frac{A_{\text{mod}}}{B^{(\aleph \text{ or } \Re)} E[I]^{(\aleph \text{ or } \Re)}}\right)^2, \quad \Phi_{j,k} = G_{7,4}^{2,6}\left(\Omega_k \left| \begin{matrix} \frac{1-\xi_{\text{mod}}^2}{2}, \frac{2-\xi_{\text{mod}}^2}{2}, \frac{1-\alpha}{2}, \frac{2-\alpha}{2}, \frac{1-j}{2}, \frac{2-j}{2}, 1 \\ 0, 0.5, -\frac{\xi_{\text{mod}}^2}{2}, \frac{1-\xi_{\text{mod}}^2}{2} \end{matrix} \right.\right)$$

and

$$\Psi_{j,k}(x) = G_{6,3}^{1,6}\left(x\Omega_k \left| \begin{matrix} \frac{1-\xi_{\text{mod}}^2}{2}, \frac{2-\xi_{\text{mod}}^2}{2}, \frac{1-\alpha}{2}, \frac{2-\alpha}{2}, \frac{1-j}{2}, \frac{2-j}{2} \\ 0, -\frac{\xi_{\text{mod}}^2}{2}, \frac{1-\xi_{\text{mod}}^2}{2} \end{matrix} \right. \right).$$

3.2 Outage Probability

For the CDMA RoFSO link, the OP for the kth user's signal is defined as the probability that the $CNIR_k(I)$ falls below a threshold value $CNIR_{k,th}$ and mathematically is expressed as [10]

$$P_{out,k} = \Pr\left(CNIR_k(I) < CNIR_{k,th}\right) = \Pr\left(I < I_{th}\right) = \int_0^{I_{th}} f_{comb,I}(I)\, dI, \tag{26}$$

where $I\text{th} = E[I]\sqrt{\frac{CNIR_{k,th}}{CNIR_{k,EX}}}$. By replacing $f_{comb,I}(I)$ with (17) and using [15, eq. (7.811.2)], we conclude to the following closed-form expression for the OP for the kth user

$$P_{out,k} = \frac{\xi_{\text{mod}}^2 A^{(\aleph \text{ or } \Re)}}{2} \sum_{j=1}^{(\aleph \text{ or } \Re)} a_j^{(\aleph \text{ or } \Re)} \left(B^{(\aleph \text{ or } \Re)}\right)^{-\frac{\alpha+j}{2}} G_{2,4}^{3,1}\left(\frac{B^{(\aleph \text{ or } \Re)} E[I]^{(\aleph \text{ or } \Re)}}{A_{\text{mod}}} \sqrt{\frac{CNIR_{k,th}}{CNIR_{k,EX}}} \left| \begin{matrix} 1, \xi_{\text{mod}}^2 + 1 \\ \xi_{\text{mod}}^2, \alpha, \beta, 0 \end{matrix} \right. \right). \tag{27}$$

4. Numerical Results

Using the derived closed-form expressions for the ABER and the OP of the RoFSO CDMA P2P link given in (25) and (27), indicative numerical results are demonstrated. We assume weak, medium, and strong turbulence conditions, specified by proper values of the Rytov variance equals to 0.1, 1.9 and 2.5, respectively. It is worth mentioning that the case of $\sigma_R^2 = 1.9$ is modeled by the gamma-gamma distribution, setting the corresponding values to the M distribution model. Finally, outcomes are presented for the case of saturated turbulence conditions with the σ_R^2 being equal to 25. In light of the above, the parameters of the M distribution model take the values of $(\sigma_R^2, \alpha, \beta, \Omega', \gamma)$ which are (0.1, 50, 14, 1.1, 0.006), (1.9, 11.29, 14, 1, 0), (2.5, 9.73, 14, 0.98, 0.02) and (25, 2.28, 33, 2.04, 0.136). It is worth noting that the parameters of the M distribution for $\sigma_R^2 = 0.1$ and 25 have been selected from [4]. Thus, taking account of the aforementioned values of σ_R^2, assuming a link distance at $L_S = 1.5$ km, an optical wavelength equal to $\lambda = 1.55$ μm, and a detector diameter $D = 2R = 10$ cm, we obtain the following values for the C_n^2 parameter, i.e., (σ_R^2, C_n^2), which are $(0.1, 2.4 \times 10^{-15}\, m^{-2/3})$, $(1.9, 4.5 \times 10^{-14}\, \text{m}^{-2/3})$, $(2.5, 6 \times 10^{-14}\, \text{m}^{-2/3})$ and $(25, 6 \times 10^{-13}\, \text{m}^{-2/3})$. The initial beam waist at the transmitter is chosen equal to $W_0 = 2.5$ cm. For the CDMA scheme, the processing gain is chosen equal to $G_p = 512$. The bandwidth for the forward link is chosen $B = 20$ MHz, while for the reverse link is $B = 10$ MHz. The IMD3 coefficient is $\alpha_3 = 1/3$, the absolute temperature is $T = 300$ K, the $RIN = -155$ dB/Hz and $P_0 = 20$ dBm. The load resistance is $R_L = 50\,\Omega$ and $< s_k(t) >= 1$. It is worth mentioning that all the user's signals are modulated with the same modulation index i.e., $m_1 = m_2 = \ldots = m_K$. The total losses for the wireless optical link are set $L_{tot} = 15$ dB.

In Fig. 3, the variation of the $CNIR_{k,EX}$ as a function of the OMI per user m_k is illustrated. It is evident that the transmission for the forward link differs significantly from that on the reverse link due to the MAI degradation. For the forward link the simultaneous transmission of 200 users is feasible, achieving a maximum $CNIR_{k,EX} = 42$ dB while for the reverse link when the channel is accessed by 10 users the maximum $CNIR_{k,EX}$ drops to a value of 26 dB. Also, it is clear that the choice of the OMI for the forward link affects the performance of the RoFSO link. In case there is a need for a specific BS to serve a large number of users, the OMI must be shifted to lower values in order to minimize IMD3 and clipping distortion. In the case of the reverse link, the choice of the

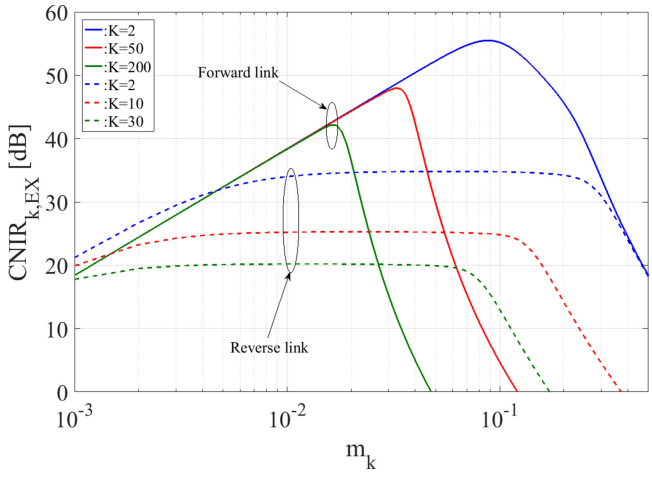

Fig. 3. Variation of the $CNIR_{k,EX}$ as a function of the OMI per user for both forward and reverse links for various values of the number of users

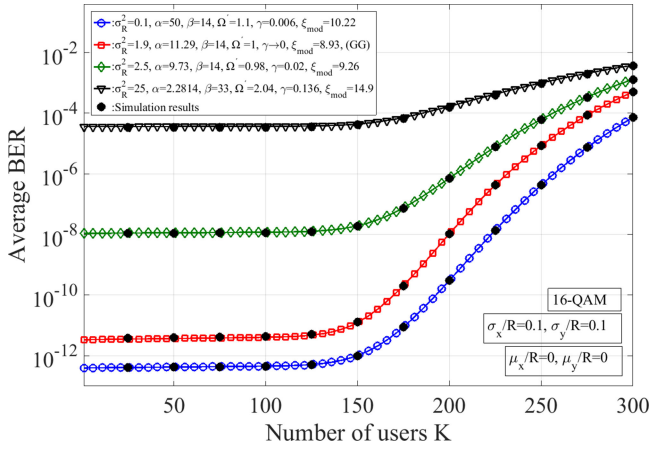

Fig. 4. The ABER for the forward link with 16-QAM for weak to strong turbulence conditions and weak PEs

optimum OMI depends on the number of users, but values in the range of $m_k = 0.01$ to 0.06 seem to be ideal.

Next in Figs. 4 and 5, results for the ABER for the forward link are depicted. The OMI per user is chosen equal to $m_k = 0.02$ and as we mentioned previously the bandwidth is set $B = 20$ MHz. The modulation format for the forward link is the 16-QAM. Due to the synchronous transmission, the number of users that simultaneously access the channel is significantly high. As it is shown, the performance aggravation occurs after the number of users exceeds the $K = 150$. Moreover, the turbulence-induced fading deteriorates the performance along with NB PEs.

In Figs. 6 and 7, the ABER results for the case of the reverse link are demonstrated. As it is obvious, the MAI on the reverse link is dominant, restricting the number of users accessing the network at a specific time instant. For the reverse link, the bandwidth is chosen $B = 10$ MHz and the OMI per user is selected equal to $m_k = 0.03$. Also, the selected modulation format is the QPSK. An acceptable performance below a BER limit of 10^{-4} is attained when the number of users is below 25 for all the cases of weak up to strong turbulence conditions. For the case of saturated turbulence conditions, when the number of active users are 3 the average BER reaches the aforementioned BER limit. The influence of the NB PEs (Fig. 7) on the ABER performance is obvious but is primarily depicted in the weak up to moderate turbulent cases.

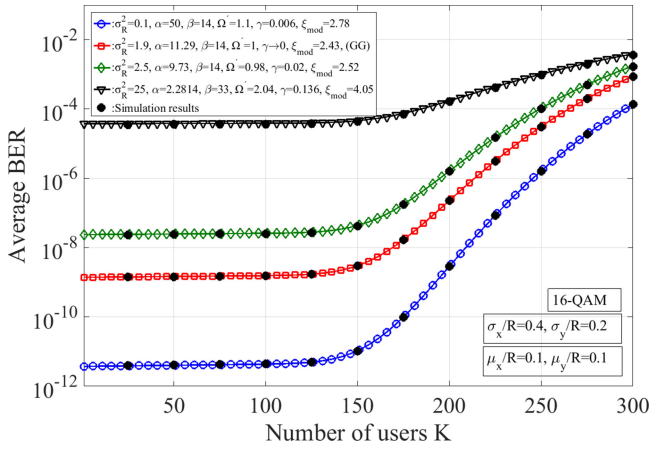

Fig. 5. The ABER for the forward link with 16-QAM for weak to strong turbulence conditions and enhanced PEs

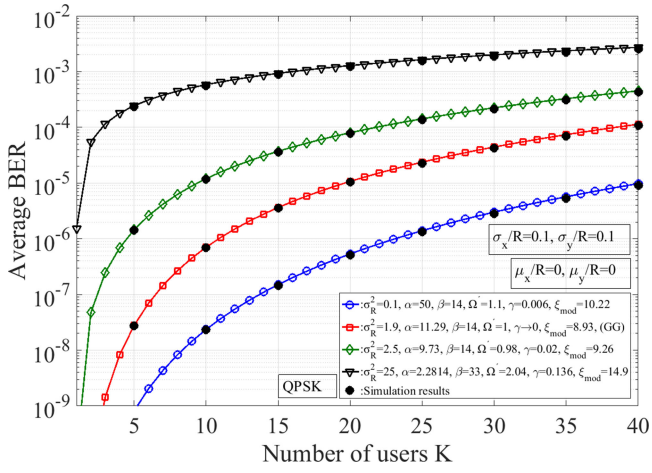

Fig. 6. The ABER for the reverse link with QPSK for weak to strong turbulence conditions and weak PEs

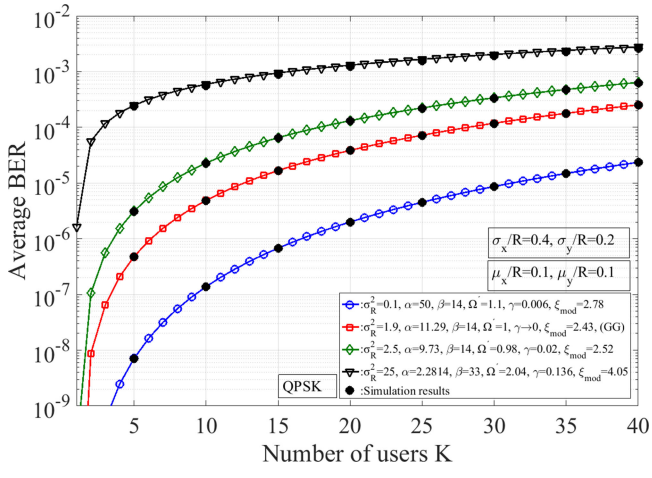

Fig. 7. The ABER for the reverse link with QPSK for weak to strong turbulence conditions and enhanced PEs.

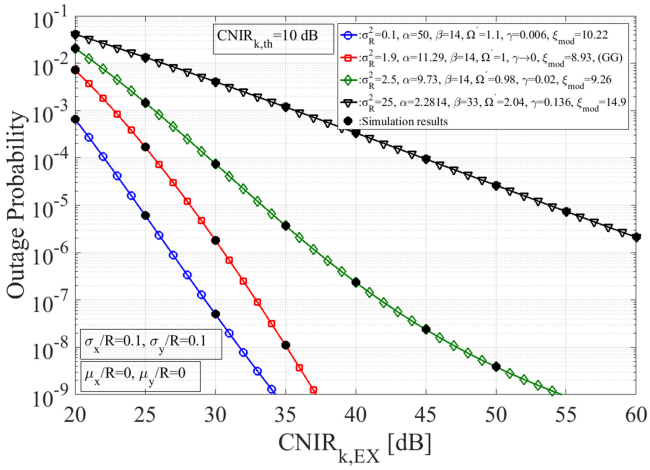

Fig. 8. The OP as a function of the $CNIR_{k,EX}$ for weak to strong turbulence conditions and weak PEs.

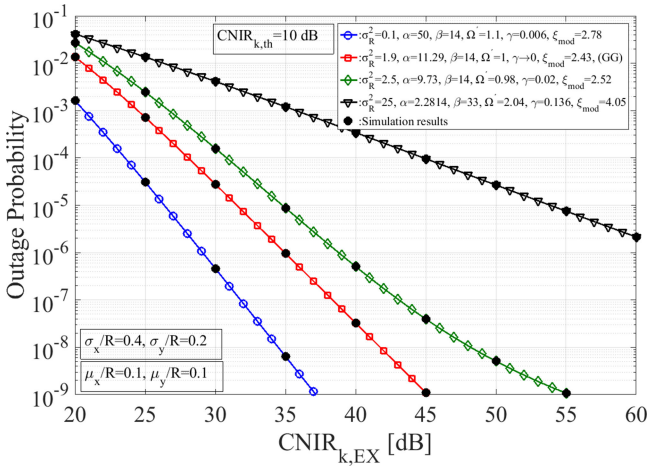

Fig. 9. The OP as a function of the $CNIR_{k,EX}$ for weak to strong turbulence conditions and enhanced PEs.

Finally, in Figs. 8 and 9, results for the OP are visualized. In this case, the numerical results are plotted as a function of the $CNIR_{k,EX}$, offering the convenience for the evaluation of the OP for both link directions. The threshold value was selected equal to $CNIR_{k,th} = 10$ dB. It is obvious that as the turbulence strength increases, the OP increases and $CNIR_k$ values above 25 dB are imperative. Also in Fig. 9, the impact of the NB displacement with enhanced spatial jitters on the OP metric is evident, especially for the weak turbulence regime.

4. Conclusions

In this paper, a CDMA RoFSO communication system is thoroughly investigated for both directions of the forward and the reverse link. Atmospheric turbulence and NB PEs were assumed, modeled by the *M*-distribution and an accurate approximation of the Beckmann distribution, respectively. In this context, novel mathematical expressions were extracted regarding the ABER and the OP of the link taking account of the aforementioned effects. Proper numerical results revealed the severe impact of the MAI and the strong influence of the atmospheric turbulence effect along with the NB PEs. In order to overcome these impediments to the performance of the CDMA RoFSO system, diversity

techniques, relay-assisted systems and error-correcting schemes seem to be indispensable and their influence could be studied in a future work.

References

[1] K. Kazaura, K. Wakamori, M. Matsumoto, T. Higashino, K. Tsukamoto, and S. Komaki, "RoFSO: A universal platform for convergence of fiber and free space optical communication networks," *IEEE Commun. Mag.*, vol. 48, no. 2, pp. 130–137, Feb. 2010.

[2] M. A. Abu-Rgheff, *Introduction to CDMA Wireless Communications*. New York, NY, USA: Academic, 2007.

[3] X. N. Fernando, *Radio over Fiber for Wireless Communications: From Fundamentals to Advanced Topics*. Hoboken, NJ, USA: Wiley-IEEE, 2014.

[4] A. Jurado-Navas, J. M. Garrido-Balsells, J. F. Paris, and A. Puerta-Notario, "A unifying statistical model for atmospheric optical scintillation," in *Numerical Simulations of Physical and Engineering Processes*, Rijeka, Croatia: Intech, 2011, pp. 181–206.

[5] R. Boluda-Ruiz, A. García-Zambrana, C. Castillo-Vázquez, and B. Castillo-Vázquez, "Novel approximation of misalignment fading modeled by Beckmann distribution on free-space optical links," *Opt. Exp.*, vol. 24, no. 20, pp. 22635–22649, 2016.

[6] A. Bekkali, P. T. Dat, K. Kazaura, K. Wakamori, and M. Matsumoto, "Performance analysis of SCM-FSO links for transmission of CDMA signals under gamma-gamma turbulent channel," in *Proc. IEEE Military Commun. Conf.*, Boston, MA, USA, Oct. 18–21, 2009, pp. 1–5.

[7] C. B. Naila, A. Bekkali, K. Wakamori, and M. Matsumoto, "Transmission analysis of CDMA-based wireless services over turbulent radio-on-FSO links using aperture averaging," in *Proc. IEEE Int. Conf. Compun.*, Kyoto, Japan, Jun. 5–9, 2011, pp. 1–6.

[8] C. B. Naila, A. Bekkali, K. Wakamori, and M. Matsumoto, "Performance analysis of CDMA-based wireless services transmission over a turbulent RF-on-FSO channel," *IEEE J. Opt. Commun. Netw.*, vol. 3, no. 5, pp. 475–486, May 2011.

[9] M. P. Ninos, H. E. Nistazakis, A. N. Stassinakis, G. S. Tombras, V. Christofilakis, and A. D. Tsigopoulos, "CDMA radio on FSO links over gamma turbulence channels with nonzero boresight pointing errors," in *Proc. 7th Int. Conf. Modern Circuits Syst. Technol.*, Thessaloniki, Greece, May 7–9, 2018, pp. 1–4.

[10] H. E. Nistazakis, A. N. Stassinakis, H. G. Sandalidis, and G. S. Tombras, "QAM and PSK OFDM RoFSO over M-turbulence induced fading channels," *IEEE Photon. J.*, vol. 7, no. 1, Feb. 2015, Art. no. 7900411.

[11] W. Huang and M. Nakagawa, "Nonlinear effect of direct-sequence CDMA in optical transmission," in *Proc. 7th IEEE Global Telecommun. Conf.*, San Francisco, CA, USA, Nov. 28, 1994–Dec. 2, 1994, pp. 1185–1189.

[12] M. B. Pursley, "Performance evaluation for phase-coded spread-spectrum multiple-access communication–part 1: System analysis," *IEEE Trans. Commun.*, vol. 25, no. 8, pp. 795–799, Aug. 1977.

[13] L. C. Andrews, R. L. Phillips, and C. Y. Hopen, *Laser Beam Scintillation With Applications*. Bellingham, WA, USA: SPIE, 2001.

[14] A. Jurado-Navas, J. M. Garrido-Balsells, J. F. Paris, M. Castillo-Vasquez, and A. Puerta-Notario, "Impact of pointing errors on the performance of generalized atmospheric optical channels," *Opt. Exp.*, vol. 20, no. 11, pp. 12550–12562, 2012.

[15] I. S. Gradshteyn and I. M. Ryzhik, *Table of Integrals, Series, and Products*, 7th ed. New York, NY, USA: Academic, 2008.

[16] A. A. Farid and S. Hranilovic, "Outage capacity optimization for free-space optical links with pointing errors," *J. Lightw. Technol.*, vol. 25, no. 7, pp. 1702–1710, Jul. 2007.

[17] I. S. Ansari, F. Yilmaz, and M. S. Alouini, "Performance analysis of free-space optical links over Málaga (M) turbulence channels with pointing errors," *IEEE Trans. Wireless Commun.*, vol. 15, no. 1, pp. 91–102, Jan. 2016.

[18] D. Sadhwani, R. N. Yadav, and S. Aggrawal, "Tighter bounds on the Gaussian Q function and its application in Nakagami-m fading channel," *IEEE Wireless Commun. Lett.*, vol. 6, no. 5, pp. 574–577, Oct. 2017.

[19] V. S. Adamchik and O. I. Marichev, "The algorithm for calculating integrals of hypergeometric type function and its realization in reduce system," in *Proc. Int. Conf. Symbolic Algebraic Comput.*, Tokyo, Japan, 1990, pp. 212–224.